Output Feedback M-MRAC Backstepping With Aerospace Applications

Vahram Stepanyan *
University of California Santa Cruz, Moffett Field, CA 94035,
Kalmanje Krishnakumar †
NASA Ames Research Center, Moffett Field, CA 94035

The paper presents a certainty equivalence output feedback backstepping adaptive control design method for the systems of any relative degree with unmatched uncertainties without over-parametrization. It uses a fast prediction model to estimate the unknown parameters, which is independent of the control design. It is shown that the system's input and output tracking errors can be systematically decreased by the proper choice of the design parameters. The approach is applied to aerospace control problems and tested in numerical simulations.

I. Introduction

Adaptive control problems are challenging for systems with unmatched uncertainties, and the majority of design methods is based on the backstepping technique outlined in Ref.[6] They become more complex when the whole state of the system is not available for feedback. It has been shown in Ref.[6] that direct application of the certainty equivalence principle leads to over-parametrization. To avoid it, nonlinear damping terms were introduced in the control design, which leads to the adaptation rate to enter into the control law. This may result in the high magnitude control signals in the case of large adaptive rates (fast adaptation), which is desirable from the perspective of the estimation of unknown parameters. An alternative certainty equivalence control design method for state feedback problems is presented in Ref.,[1] which avoids over parametrization for linear systems, but the method is only applicable for nonlinear systems with the relative degree not exceeding two.

In Ref.,[11] we introduced a certainty equivalence state feedback indirect adaptive control approach without over parametrization for nonlinear systems of any relative degree. The approach was based on the state prediction model, which is capable of providing fast estimation of unknown parameters independent of the control design. This property is the consequence of feeding back an error term with the gain proportional to the square root of the adaptation rate, like in the modified reference model MRAC (M-MRAC) architecture introduced in Ref.,[10] where it has been shown that the error feedback gain acts as a damping factor for the adaptive signals, whereas the adaptation rate determines its frequency. In this paper we extend the method to the systems in parametric output feedback form. This extension uses conventional filtering approach to transform the system into the form suitable for the parameter estimation. The control design uses the prediction model's and the filter's states, and follows the command filtered backstepping procedure from Ref.[2] It is shown that the input tracking error (difference between ideal control and command filtered certainty equivalence control signal) and output tracking error can be regulated as desired by the proper choice of design parameters.

The rest of the paper is organized as follows. In Section II, we give the problem statement, main assumptions and input-output filtered transformations. In Section III, we introduce the identification model and give its properties. The control design and performance analysis are presented in Section IV. Aerospace applications are presented in Section V, and some concluding remarks are given in Section VI.

*Senior Research Scientist, University Affiliated Research Center, Senior Member AIAA, vahram.stepanyan@nasa.gov
†Autonomous Systems and Robotics Branch Chief, Intelligent Systems Division, Associate Fellow AIAA, kalmanje.krishnakumar@nasa.gov

II. Problem Statement

Consider an uncertain single input single output (SISO) system in the parametric output feedback form[6] (p. 99)

$$\begin{aligned} \dot{\boldsymbol{x}}(t) &= A_n \boldsymbol{x}(t) + \boldsymbol{f}(y) + \Phi(y)\boldsymbol{\theta} + \boldsymbol{d}u(t) \\ y(t) &= \boldsymbol{c}_n^\top \boldsymbol{x}(t)\,, \end{aligned} \tag{1}$$

with some initial conditions $\boldsymbol{x}(0) = \boldsymbol{x}_0$, where $\boldsymbol{x} \in \mathbb{R}^n$, $u \in \mathbb{R}$ and $y \in \mathbb{R}$ are the state, input and output of the system, $\boldsymbol{\theta} \in \mathbb{R}^p$ is a vector of unknown constant parameters, $\boldsymbol{f} : \mathbb{R} \to \mathbb{R}^n$ and $\Phi : \mathbb{R} \to \mathbb{R}^{n\times p}$ are sufficiently smooth known functions, and $A_n,\ \boldsymbol{d},\ \boldsymbol{c}_n$ have forms

$$A_n = \begin{bmatrix} 0_{(n-1)\times 1} & \mathbb{I}_{(n-1)\times(n-1)} \\ 0 & 0_{1\times(n-1)} \end{bmatrix},\ \boldsymbol{d} = \begin{bmatrix} 0_{(n-m+1)\times 1} \\ d_m \\ \vdots \\ d_0 \end{bmatrix},\ \boldsymbol{c}_n = \begin{bmatrix} 1 \\ 0_{(n-1)\times 1} \end{bmatrix}$$

It is assumed that $\boldsymbol{d}$ is unknown, d_m is positive and bounded below by a known constant d_*, and the polynomial $d_m s^m + \cdots + d_1 s + d_0$ is known to be Hurwitz.

The objective is to design a control signal $u(t)$ using only the output $y(t)$ such that all closed-loop signals are bounded, and $y(t)$ tracks the output $y_r(t) = \boldsymbol{c}^\top \boldsymbol{x}_r(t)$ of the reference model

$$\dot{\boldsymbol{x}}_r(t) = \bar{A}\boldsymbol{x}_r(t) + \bar{\boldsymbol{b}}r(t), \quad \boldsymbol{x}_r(0) = \boldsymbol{x}_0\,, \tag{2}$$

where $\boldsymbol{x}_r \in \mathbb{R}^q$ $(q = n - m)$ is the state of the model, $r(t)$ is a piece-wise continuous and bounded external command, $\bar{A} = A_q - \boldsymbol{b}_q\boldsymbol{k}^\top$, $\bar{\boldsymbol{b}} = k\boldsymbol{b}_q$. Here we denote $\boldsymbol{b}_q = [0_{(q-1)\times 1}\ 1]^\top$, and the gains $\boldsymbol{k}$ and k are chosen to make $\bar{A}$ Hurwitz and meet the performance specifications.

Following the steps from Ref.[6] (p.329), we transform the system (1) by means of the filters introduced in Ref.[5] In this particular case these filters take the form

$$\begin{aligned} \dot{\boldsymbol{s}}(t) &= A_0\boldsymbol{s}(t) + \boldsymbol{k}_0 y(t) + \boldsymbol{f}(y) \\ \dot{\Xi}(t) &= A_0\Xi(t) + \Phi(y) \\ \dot{\boldsymbol{\mu}}(t) &= A_0\boldsymbol{\mu}(t) + \boldsymbol{b}_n u(t)\,, \end{aligned} \tag{3}$$

where the constant vector $\boldsymbol{k}_0$ is chosen such that the matrix $A_0 = A_n - \boldsymbol{k}_0\boldsymbol{c}_n^\top$ is Hurwitz. It is straightforward to show that

$$\boldsymbol{x}(t) = \boldsymbol{s}(t) + \Xi(t)\boldsymbol{\theta} + \sum_{i=0}^{m} d_i \boldsymbol{w}_i(t) + \boldsymbol{\delta}(t)\,, \tag{4}$$

where $\boldsymbol{w}_i(t) = A_0^i\boldsymbol{\mu}(t),\ i = 0, \ldots, m$, and $\boldsymbol{\delta}(t)$ is a solution of the exponentially stable system

$$\dot{\boldsymbol{\delta}}(t) = A_0\boldsymbol{\delta}(t)\,. \tag{5}$$

In Ref.,[6] $\boldsymbol{\delta}(t)$ was treated as a bounded external disturbance, and a nonlinear damping term was added in the control signal to compensate for it. Here, we show that the certainty equivalent controller can achieve the objective without extra terms or over-parametrization.

Using the representation (4) we transform the output dynamics as follows

$$\begin{aligned} \dot{y}(t) &= x_2(t) + f_1(y) + \Phi_{(1)}(y)\boldsymbol{\theta} \\ &= s_2(t) + \Xi_{(2)}(t)\boldsymbol{\theta} + \sum_{i=0}^{m} d_i w_{i,2}(t) + \delta_2(t) + f_1(y) + \Phi_{(1)}(y)\boldsymbol{\theta} \\ &= d_m w_{m,2}(t) + f_1(y) + s_2(t) + \boldsymbol{h}^\top(t)\boldsymbol{\vartheta} + \delta_2(t)\,, \end{aligned} \tag{6}$$

where $\Xi_{(2)}(t)$ denotes the second column of matrix $\Xi(t)$, $\boldsymbol{\vartheta} = [d_{m-1}\ \ldots\ d_0\ \boldsymbol{\theta}^\top]^\top$ is the augmented vector of unknown parameters, and $\boldsymbol{h}(t) = [w_{m-1,2}(t)\ \ldots\ w_{0,2}(t)\ \ \Xi_{(2)}(t) + \Phi_{(1)}(y)]^\top$ is the augmented vector of

regressors. Combining (6) with the $\boldsymbol{w}_m$-dynamics we obtain a q-dimensional system for the control design

$$\begin{aligned}\dot{y}(t) &= d_m w_{m,2}(t) + f_1(y) + s_2(t) + \boldsymbol{h}^\top(t)\boldsymbol{\vartheta} + \delta_2(t)\\ \dot{w}_{m,j}(t) &= w_{m,j+1}(t) - k_j w_{m,1}(t), \quad j = 2,\ldots,q-1\\ \dot{w}_{m,q}(t) &= u(t) + w_{m,q+1}(t) - k_q w_{m,1}(t)\,.\end{aligned} \tag{7}$$

Obviously (7) is in parametric output feedback form, the states of which are available for the control design. Therefore, the state feedback M-MRAC backstepping approach from the Ref.[11] can be applied. The difference is the presence of the unknown virtual control confficient d_m. Since the control law will contain division by the estimate of d_m, a projection operator can be employed to bound it away from zero using the available lower limit d_*.

III. Identification Model

Since the uncertainties are lumped in the first equation of (7), we use a reduced order identification model to estimate the unknown parameters

$$\begin{aligned}\dot{\hat{y}}(t) &= \hat{d}_m(t) w_{m,2}(t) + f_1(y) + s_2(t) + \boldsymbol{h}^\top(t)\hat{\boldsymbol{\vartheta}}(t) + \lambda\tilde{y}(t)\\ \hat{y}(0) &= \hat{y}_0\,,\end{aligned} \tag{8}$$

where $\hat{y}(t)$ is the output prediction, $\tilde{y}(t) = y(t) - \hat{y}(t)$ is the output prediction error, $\lambda > 0$ is a design parameter, $\hat{d}_m(t)$ and $\hat{\boldsymbol{\vartheta}}(t)$ are the estimates of the unknown parameters, which are generated according to adaptive laws

$$\begin{aligned}\dot{\hat{d}}_m(t) &= \gamma\,\mathrm{Pr}\left(\hat{d}_m(t), \tilde{y}(t) w_{m,2}(t)\right)\\ \dot{\hat{\boldsymbol{\vartheta}}}(t) &= \gamma\tilde{y}(t)\boldsymbol{h}(t)\,,\end{aligned} \tag{9}$$

where $\gamma > 0$ is the adaptation rate and $\mathrm{Pr}(\cdot,\cdot)$ denotes the projection operator (see Ref.[8] for details).

The output prediction error dynamics do not explicitly depend on the control signal

$$\dot{\tilde{y}}(t) = -\lambda\tilde{y}(t) + \tilde{\eta}(t) + \delta_2(t)\,, \tag{10}$$

where we define $\tilde{\eta}(t) \equiv \eta(t) - \hat{\eta}(t) = d_m w_{m,2}(t) + \boldsymbol{h}^\top(t)\boldsymbol{\vartheta} - \hat{d}_m(t) w_{m,2}(t) - \boldsymbol{h}^\top(t)\hat{\boldsymbol{\vartheta}}(t) = \tilde{d}_m(t) w_{m,2}(t) + \boldsymbol{h}^\top(t)\tilde{\boldsymbol{\vartheta}}(t)$ with $\tilde{d}_m(t) = d_m - \hat{d}_m(t)$ and $\tilde{\boldsymbol{\vartheta}}(t) = \boldsymbol{\vartheta} - \hat{\boldsymbol{\vartheta}}(t)$ being the parameter estimation errors.

The following properties of the identification model can be established.

Lemma III.1 *The error signals $\tilde{y}(t)$, $\tilde{d}_m(t)$ and $\tilde{\boldsymbol{\vartheta}}(t)$ are globally uniformly bounded, and $\tilde{y}(t) \to 0$ as $t \to \infty$.*

Proof. Consider a candidate Lyapunov function

$$V(t) = \tilde{y}^2(t) + \frac{1}{\gamma}\tilde{d}_m^2(t) + \frac{1}{\gamma}\tilde{\boldsymbol{\vartheta}}^\top(t)\tilde{\boldsymbol{\vartheta}}(t) + \boldsymbol{\delta}^\top(t) P \boldsymbol{\delta}(t)\,, \tag{11}$$

where P is the positive definite solution of the Lyapunov equation $A_0^\top P + P A_0 = -Q$ for a given positive definite matrix Q. It is straightforward to compute the derivative of $V(t)$ along the trajectories of the prediction error dynamics (10) and the adaptive laws (9). Using the properties of the projection operator (see for example Ref.[8]) we obtain the inequality

$$\dot{V}(t) \le -2\lambda\tilde{y}^2(t) + 2\tilde{y}(t)\delta_2(t) - \boldsymbol{\delta}^\top(t) Q \boldsymbol{\delta}(t)\,. \tag{12}$$

Completing the squares we arive at

$$\dot{V}(t) \le -(2\lambda - 1)\tilde{y}^2(t) - (\lambda_{\min}(Q) - 1)\|\boldsymbol{\delta}(t)\|^2\,. \tag{13}$$

Choosing $\lambda_{\min}(Q) > 1$ and $2\lambda > 1$, we conclude from the LaSalle-Yoshizawa theorem (,[6] p.24) that $\tilde{y}(t)$, $\tilde{d}_m(t)$ and $\tilde{\boldsymbol{\vartheta}}(t)$ are globally uniformly bounded, and $\tilde{y}(t) \to 0$ as $t \to \infty$. In particular, there exists $\beta_1 > 0$ such that $|\tilde{d}_m^2(t)| + \|\tilde{\boldsymbol{\vartheta}}(t)\|^2 \le \beta_1^2$.

The next lemma gives the bound on the output prediction error.

Lemma III.2 *$\tilde{y}(t)$ satisfies the bound*

$$|\tilde{y}(t)| \leq \beta_2 e^{-\nu_0 t} + \frac{\beta_1}{\sqrt{\gamma}}, \tag{14}$$

where $\beta_2 = \sqrt{|2V(0) - \frac{\beta_1^2}{\gamma}|}$ and $\nu_0 = \min(\lambda_{\min}(Q) - 1,\ 2\lambda - 1)$.

Proof. It is easy to see that the inequality (13) can be written as

$$\dot{V}(t) \leq -\nu_0 V(t) + \frac{\nu_0}{\gamma}\beta_1^2, \tag{15}$$

which implies that

$$V(t) \leq \left[V(0) - \frac{\beta_1^2}{2\gamma}\right] e^{-\nu_0 t} + \frac{\beta_1^2}{2\gamma}. \tag{16}$$

Recalling that $\|\tilde{y}(t)\|^2 \leq 2V(t)$, we obtain

$$\|\tilde{y}(t)\| \leq \sqrt{\left[2V(0) - \frac{\beta_1^2}{\gamma}\right] e^{-\nu_0 t} + \frac{\beta_1^2}{\gamma}}, \tag{17}$$

The bound (14) follows from the fact that $\sqrt{a+b} \leq \sqrt{a} + \sqrt{b}$ for any $a \geq 0,\ b \geq 0$.

When $y(t)$ and $u(t)$ are bounded (which will be provided by the control design), a tighter bound on $\tilde{y}(t)$ can be derived through the bound on the adaptive error signal $\tilde{\boldsymbol{\eta}}(t)$, which is given by the following lemma.

Lemma III.3 *Let the estimates $\hat{y}(t)$ and $\hat{\boldsymbol{\vartheta}}(t)$ be generated by the identification model (8) and (9). In addition, let $y(t)$ and $u(t)$ be bounded. Then $\tilde{\eta}(t)$ and $\tilde{y}(t)$ satisfy the following bounds*

$$|\tilde{\eta}(t)| \leq \beta_3 e^{-\nu t} + \tfrac{\beta_4}{\sqrt{\gamma}} \tag{18}$$

$$|\tilde{y}(t)| \leq \beta_5 e^{-\nu t} + \tfrac{\beta_6}{\lambda\sqrt{\gamma}}, \tag{19}$$

where the constants $\beta_i > 0,\ i = 3, \ldots, 6$ and $\nu_1 > 0$ are defined in the proof.

Proof. Following Ref.,[10] it is straightforward to show that $\tilde{\eta}(t)$ satisfies the dynamics

$$\ddot{\tilde{\eta}}_i(t) + \lambda\dot{\tilde{\eta}}_i(t) + \gamma\rho(t)\tilde{\eta}_i(t) = -\gamma\dot{\rho}(t)\tilde{y}(t) + c r_a(t) + \dot{r}_a(t) - \gamma\rho(t)\delta_2(t), \tag{20}$$

where $\rho(t) = w_{m,2}^2(t) + \boldsymbol{h}^\top(t)\boldsymbol{h}(t)$, $r_a(t) = \tilde{b}_m(t)\dot{w}_{m,2}(t) + \tilde{\boldsymbol{\vartheta}}^\top(t)\dot{\boldsymbol{h}}(t)$. Since $y(t)$ and $u(t)$ are bounded, and $\boldsymbol{f}(y),\ \Phi(y)$ are smooth functions, $\boldsymbol{s}(t)$, $\boldsymbol{\mu}(t)$ and $\Xi(t)$ are bounded. These imply that $w_{m,2}(t)$, $\boldsymbol{h}(t)$ and $y(t)$ are bounded. Also, it follows from (6) that $\dot{y}(t)$ is bounded, which implies that $\dot{w}_{m,2}(t)$, $\dot{\boldsymbol{h}}(t)$ are bounded as well. Therefore, there exist positive constants $c_1,\ c_2,\ c_3$ such that $\|\rho(t)\|_{\mathcal{L}_\infty} \leq c_1$, $\|\dot{\rho}(t)\|_{\mathcal{L}_\infty} \leq c_2$ and $\|r_a(t)\|_{\mathcal{L}_\infty} \leq c_3$. On the other hand $\delta_2(t)$ satisfies the bound $|\delta_2(t)| \leq c_4 e^{-\nu_1 t}$, where $c_4 > 0$ depends on the initial conditions and ν_1 is the decay rate of the Hurwitz matrix A_0. Then, it follows from the results of Ref.[10] that choosing $\lambda \geq 2\sqrt{c_1\gamma}$ damps the oscillations in $\tilde{\eta}(t)$ and guarantees the bound

$$|\tilde{\eta}(t)| \leq \beta_3 e^{-\nu t} + c_2|\tilde{y}(t)| + \frac{c_5}{\sqrt{\gamma}}|r_a(t)|, \tag{21}$$

where $\nu = \min(\nu_0,\ \nu_1,\ \nu_2)$, ν_2 is proportional to $\sqrt{\gamma}$, and the positive constants β_3 and c_4 are independent of γ (see details in[10]). Substituting (14) we arrive to (18) with $\beta_4 = c_2\beta_1 + c_3 c_5$.

A tighter bound on $\tilde{y}(t)$ is obtained from (10) by direct integration.

$$|\tilde{y}(t)| \leq \frac{\beta_3}{\lambda - \nu}\left[e^{-\nu t} - e^{-\lambda t}\right] + \frac{c_4}{\lambda - \nu_1}\left[e^{-\nu_1 t} - e^{-\lambda t}\right] + \frac{\beta_4}{\lambda\sqrt{\gamma}}\left[1 - e^{-\lambda t}\right] \leq \beta_5 e^{-\nu t} + \frac{\beta_6}{\lambda\sqrt{\gamma}}, \tag{22}$$

since $\nu_1 > \nu$ by definition and $\lambda > \nu$ for fast adaptation.

IV. Control Design

In this section, we first design a conventional backstepping controller for the known system (ideal controller), which is used only for analysis purposes, then design the command filtered certainty equivalence controller, which is actually being implemented.

A. Known System

We follow the standard backstepping procedure from Ref.[6] and design the ideal controller for the system (7) ignoring the term $\delta_2(t)$. The reason is that the actual control signal is defined using the identification model, which does not evolve that term. Let the error variables be defined as

$$e_1^0(t) = y^0(t) - y_r(t) \tag{23}$$

$$e_i^0(t) = w_{m,i}^0(t) - \alpha_{i-1}^0(t), \quad i = 2, \dots, q\,, \tag{24}$$

where the stabilizing functions $\alpha_i^0(t),\ i = 1, \dots, q-1$ have the form

$$\alpha_1^0(t) = \tfrac{1}{d_m}[-ce_1^0(t) - f_1(y^0) - s_2^0(t) - \boldsymbol{h}^{0\top}(t)\boldsymbol{\vartheta} + x_{r,2}(t)] \tag{25}$$

$$\alpha_2^0(t) = -d_m e_1^0(t) - c_2 e_2^0(t) + k_2 w_{m,1}^0(t) + \dot{\alpha}_1^0(t) \tag{26}$$

$$\alpha_i^0(t) = -e_{i-1}^0(t) - c_i e_i^0(t) + k_i w_{m,1}^0(t) + \dot{\alpha}_{i-1}^0(t), \quad i = 3, \dots, q-1\,.$$

with $c_i > 0,\ i = 1, \dots, q-1$ being design parameters. Here and in the following derivations, the superscript 0 indicates that the variables correspond to the ideal case. We define the ideal control signal as

$$u^0(t) = -e_{i-1}^0(t) - c_q e_q^0(t) - w_{m,q+1}^0(t) + k_q w_{m,1}^0(t) + \dot{\alpha}_{q-1}^0(t)\,, \tag{27}$$

It is easy to see that the error system has the form

$$\dot{\boldsymbol{e}}^0(t) = A_{id}\boldsymbol{e}^0(t)\,, \tag{28}$$

where

$$A_{id} = \begin{bmatrix} -c_1 & d_m & 0 & 0 & \dots & 0 \\ -d_m & -c_2 & 1 & 0 & \dots & 0 \\ 0 & -1 & -c_3 & 1 & \dots & 0 \\ \vdots & \vdots & \vdots & \vdots & \ddots & \vdots \\ 0 & 0 & 0 & 0 & \dots & -c_q \end{bmatrix}.$$

Therefore it is exponentially stable. That is, $y^0(t) = y_r(t) + e_1^0(t)$ exponentially converges to $y_r(t)$. In addition, from $r(t) \in \mathcal{L}_\infty$ it follows that $\boldsymbol{x}_r(t) \in \mathcal{L}_\infty$, which along with $\boldsymbol{e}^0(t) \in \mathcal{L}_\infty$ can be used to recursively show that $\alpha_i^0(t),\ \dot{\alpha}_i^0(t),\ i = 1, \dots, q-1,\ w_{m,i},\ i = 1, \dots, q+1$ are bounded. Then, $u^0(t) \in \mathcal{L}_\infty$ is bounded, and the boundedness of $\boldsymbol{\mu}(t)$ and hence all closed-loop signals follow.

B. Command Filtering Certainty Equivalent Control

Here, we use command filtering approach from Ref.[2] and design a certainty equivalence control for the identification model augmented with the last $q-1$ equations in (7).

The uncompensated errors are introduced as

$$e_1(t) = \hat{y}(t) - y_r(t) \tag{29}$$

$$e_i(t) = w_{m,i}(t) - \sigma_{i-1,1}(t), \quad i = 2, \dots, q\,, \tag{30}$$

where $\sigma_{i-1,1}(t)$ is the first state of the second order LTI system, which is used to filter the stabilizing functions. Here, these functions are defined as

$$\alpha_1(t) = \frac{1}{\hat{d}_m(t)}[-ce_1(t) - f_1(y) - s_2(t) - \boldsymbol{h}^\top(t)\boldsymbol{\vartheta} + x_{r,2}(t)] \tag{31}$$

$$\alpha_2(t) = -\hat{d}_m(t)e_1(t) - c_2 e_2(t) + k_2 w_{m,1}(t) + \omega\sigma_{1,2}(t) \tag{32}$$

$$\alpha_i(t) = -e_{i-1}(t) - c_i e_i(t) + k_i w_{m,1}(t) + \omega\sigma_{i-1,2}(t), \quad i = 3, \dots, q-1\,,$$

where $\sigma_{i-1,2}(t)$ is the second state of the filter's dynamics, which is given by the equations

$$\begin{aligned}\dot{\sigma}_{i,1}(t) &= \omega\sigma_{i,2}(t) \\ \dot{\sigma}_{i,2}(t) &= -2\zeta\omega\sigma_{i,2}(t) - \omega[\sigma_{i,1}(t) - \alpha_i(t)] \\ & i = 1, \ldots, n-1\,,\end{aligned} \tag{33}$$

with the initial conditions $\sigma_{i,1}(0) = \alpha_i(0)$ and $\sigma_{i,2}(0) = 0$.

The compensated errors are introduced as $\boldsymbol{e}^c(t) = \boldsymbol{e}(t) - \boldsymbol{\xi}(t)$, where $\boldsymbol{\xi}(t)$ is dynamically defined as

$$\begin{aligned}\dot{\xi}_1(t) &= \sigma_{1,1}(t) - \alpha_1(t) + \xi_2(t) \\ \dot{\xi}_i(t) &= \sigma_{i,1}(t) - \alpha_i(t) + \xi_{i+1}(t), \quad i = 2, \ldots, n-1\end{aligned} \tag{34}$$

with $\xi_i(0) = 0$ for $i = 1, \ldots, n-1$, and $\xi_n(t) \equiv 0$. These modifications lead to the definition of the actual control signal as

$$u(t) = -e^c_{i-1}(t) - c_q e^c_q(t) - w_{m,q+1}(t) + k_q w_{m,1}(t) + \omega\sigma_{q-1,2}(t)\,. \tag{35}$$

The resulting compensated error dynamics are given by the equation

$$\dot{\boldsymbol{e}}^c(t) = \hat{A}(t)\boldsymbol{e}^c(t) + \lambda \boldsymbol{c}_q \tilde{y}(t)\,, \tag{36}$$

where $\hat{A}(t)$ is obtained from A_{id} by replacing d_m with its estimate $\hat{d}_m(t)$. Obviously, the error system (36) is asymptotically stable, since $\tilde{y}(t) \to 0$ as $t \to \infty$ according to Section III. On the other hand, the uncompensated error $\boldsymbol{e}(t)$ has dynamics

$$\dot{\boldsymbol{e}}(t) = \hat{A}(t)\boldsymbol{e}(t) - \bar{\boldsymbol{\alpha}}(t) + \bar{\boldsymbol{\sigma}}(t) + \lambda \boldsymbol{c}_q \tilde{y}(t)\,. \tag{37}$$

where

$$\bar{\boldsymbol{\alpha}}(t) = \begin{bmatrix} \hat{d}_m(t)\alpha_1(t) \\ \vdots \\ \alpha_{q-1}(t) \\ 0 \end{bmatrix},\ \bar{\boldsymbol{\sigma}}(t) = \begin{bmatrix} \hat{d}_m(t)\sigma_{1,1}(t) \\ \vdots \\ \sigma_{q-1,1}(t) \\ 0 \end{bmatrix}.$$

The performance of the designed controller is given by the following theorem, the proof of which can be carried out following the steps from Ref.[11]

Theorem IV.1 *Let the controller be defined according to identification model (8), adaptive law (9), and command filtered backstepping scheme given by (29), (31), (33), (34) and (35). Then the input and output tracking errors satisfy the following upper bounds*

$$|u(t) - u^0(t)| \le \beta_7 e^{-\nu_3 t} + \tfrac{\beta_8}{\sqrt{\gamma}} + \mathcal{O}(\varepsilon) \tag{38}$$

$$|y(t) - y_r(t)| \le \beta_9 e^{-\nu_3 t} + \tfrac{\beta_{10}}{\sqrt{\gamma}} + \mathcal{O}(\varepsilon)\,, \tag{39}$$

where β_7, β_8, β_9, β_{10} are positive constants independent of γ, ν_3 is the decay rate of the reference model, $\varepsilon = 1/\omega$ (the proper choice of ζ and ω is discussed in Ref.[2]), and the notation $\mathcal{O}(\varepsilon)$ is adopted from Ref.[4] (p. 383).

V. Aerospace Applications

A. Control of Wing Rock

We consider a wing rock motion of a slender delta wing, which is given by the equation

$$\ddot{\phi}(t) = f(\phi, \dot{\phi}) + b_a \delta_a(t)\,.$$

where $\phi(t)$ is the roll angle, $\delta_a(t)$ is the aileron deflection and $f(\phi, \dot{\phi})$ has the form (see Ref.[9] for details)

$$f(\phi, \dot{\phi}) = \theta_1\phi + \theta_2\dot{\phi} + \theta_3|\phi^2|\dot{\phi} + \theta_4|\dot{\phi}|\dot{\phi} + \theta_5\phi^3 \equiv \boldsymbol{\theta}^\top \boldsymbol{\varphi}(\phi, p)\,. \tag{40}$$

Modeling ailerons as a first order dynamics

$$\tau\dot{\delta}_a(t) \quad = \quad u(t) - \delta_a(t)\,, \tag{41}$$

where τ is the ailerons time constant, and introducing a new variable $x_3(t) = b_a\delta_a(t)$, we represent the system in the state space form as

$$\begin{aligned} \dot{x}_1(t) &= x_2(t) \\ \dot{x}_2(t) &= x_3(t) + \boldsymbol{\theta}^\top \boldsymbol{\varphi}(x_1, x_2) \\ \dot{x}_3(t) &= -kx_3(t) + bu(t)\,, \end{aligned} \tag{42}$$

where $x_1(t) = \phi(t)$ denotes the roll angle, $x_2(t) = p(t)$ denotes the roll rate, $k = \frac{1}{\tau}$ is assumed to be known, $b = \frac{b_a}{\tau}$ is assumed to be unknown, and $u(t)$ is the control signal to be designed assuming that $x_1(t)$ and $x_2(t)$ are available for feedback.

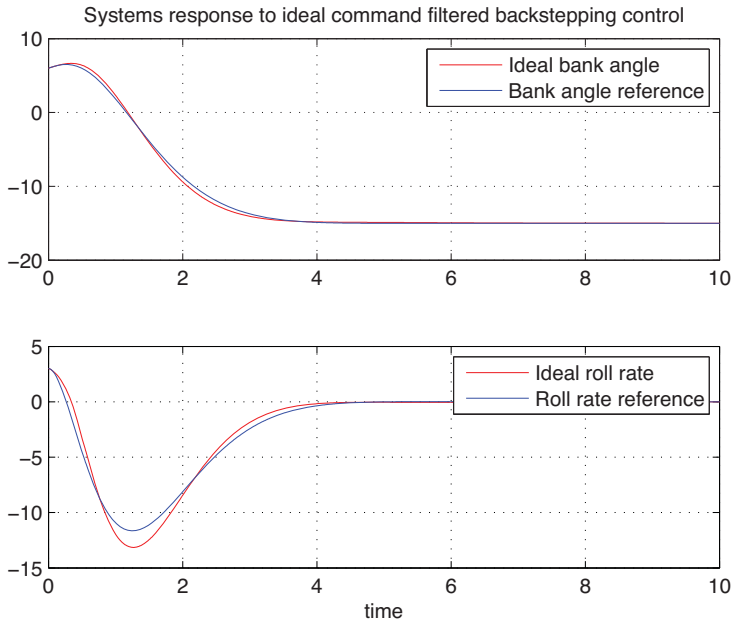

Figure 1. Step response to the ideal command filtered output feedback control.

The system consists of two blocks. First contains only the first equation, which is free of uncertainties, the second consists of the last two equations, which contain unknown parameters. Since x_3 is not accessible, we transform the second block into the parametric output feedback form using a linear transformation

$$\begin{aligned} z_2(t) &= x_2(t) \\ z_3(t) &= kx_2(t) + x_3(t)\,. \end{aligned} \tag{43}$$

The transformed system has a form

$$\begin{aligned} \dot{z}_1(t) &= z_2(t) \\ \dot{z}_2(t) &= z_3(t) - kz_2(t) + \boldsymbol{\theta}^\top \boldsymbol{\varphi}(x_1, x_2) \\ \dot{z}_3(t) &= bu(t) + k\boldsymbol{\theta}^\top \boldsymbol{\varphi}(x_1, x_2)\,, \end{aligned} \tag{44}$$

where for uniformity we also introduce $z_1(t) = x_1(t)$. Using the filtered transformation (46) we write the system as

$$\begin{aligned} \dot{z}_1(t) &= z_2(t) \\ \dot{z}_2(t) &= b\mu_2(t) + s_2(t) - kz_2(t) + \boldsymbol{\vartheta}^\top \boldsymbol{h}(t) \\ \dot{\mu}_2(t) &= u(t) - k_{02}\mu_1(t)\,, \end{aligned} \tag{45}$$

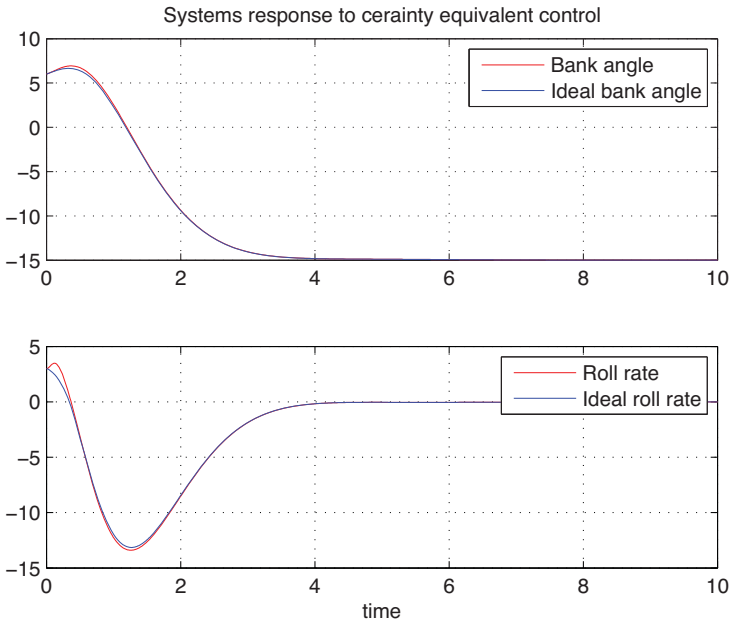

Figure 2. Step response of the certainty equivalent control.

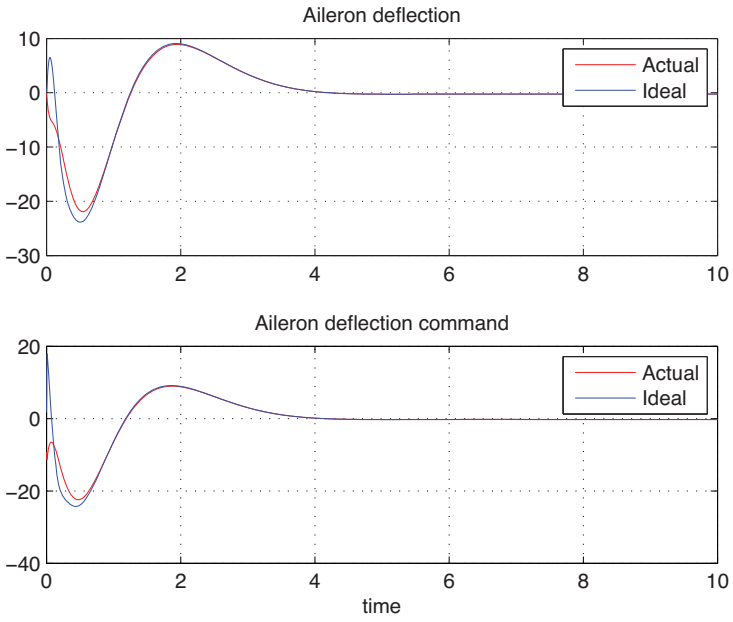

Figure 3. Actual aileron deflection and certainty equivalent adaptive control signal vs ideal ones for the step command.

where $\boldsymbol{h}(t) = [\Xi_{(2)}(t) + \boldsymbol{\varphi}^\top(x_1, x_2) \;\; \psi_1(t) \;\; \psi_2(t)]^\top$, and $\boldsymbol{s}(t)$, $\Xi(t)$, $\boldsymbol{\mu}(t)$ are generated according to equations

$$\dot{\boldsymbol{s}}(t) = A_0 \boldsymbol{s}(t) + \begin{bmatrix} k_{0,1} - k \\ k_{0,2} \end{bmatrix} x_2(t), \quad \dot{\Xi}(t) A_0 \Xi(t) + \begin{bmatrix} \boldsymbol{\varphi}^\top(x_1, x_2) \\ k\boldsymbol{\varphi}^\top(x_1, x_2) \end{bmatrix}, \quad \dot{\boldsymbol{\mu}}(t) = A_0 \boldsymbol{\mu}(t) + \begin{bmatrix} 0 \\ 1 \end{bmatrix} u(t)\,, \quad (46)$$

where

$$A_0 = \begin{bmatrix} -k_{0,1} & 1 \\ -k_{0,2} & 0 \end{bmatrix}$$

The identification model is introduced for the z_2-dynamics, where the uncertainties are lumped in.

$$\dot{\hat{z}}_2(t) = \hat{b}(t)\mu_2(t) + s_2(t) - kz_2(t) + \hat{\boldsymbol{\vartheta}}^\top(t)\boldsymbol{h}(t) + \lambda[z_2(t) - \hat{z}_2(t)]\,, \tag{47}$$

where the estimates $\hat{b}(t)$ and $\hat{\boldsymbol{\vartheta}}^\top(t)$ are generated according to adaptive laws (9).

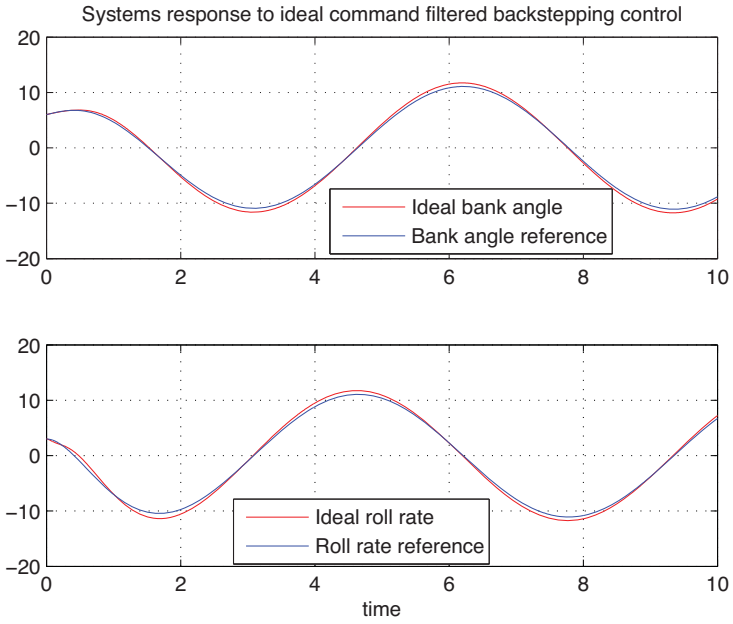

Figure 4. Sinusoidal response of the ideal command filtered output feedback control.

In the first step of the control design we introduce the error $e_1(t) = y(t) - y_r(t) = z_1(t) - x_{r,1}(t)$ and the stabilizing function $\alpha_1(t) = -c_1(t)e_1(t) + x_{r,2}$, which results in

$$\dot{e}_1(t) = -c_1 e_1(t) + e_2(t) + \tilde{z}_2(t)\,, \tag{48}$$

where $e_2(t) = \hat{z}_2(t) - \alpha_1(t)$. Since differentiation of $\alpha_1(t)$ involves only linear terms, we do not use command filtering in this step. This results into the equation

$$\dot{e}_2(t) = \hat{b}(t)\mu_2(t) + s_2(t) - kz_2(t) + \hat{\boldsymbol{\vartheta}}^\top(t)\boldsymbol{h}(t) - x_{r,3} - c_1^2 e_1(t) + c_1 e_2(t) + (\lambda + c_1)\tilde{z}_2(t)\,. \tag{49}$$

The stabilizing function $\alpha_2(t)$ is modified to include a term $-e_1(t)$ to counteract the effect of the error term $e_2(t)$ in (48), and has the form

$$\alpha_2(t) = \frac{1}{\hat{b}(t)}\left[(c_1^2 - 1)e_1(t) - (c_1 + c_2)e_2(t) - s_2(t) + kz_2(t) - \hat{\boldsymbol{\vartheta}}^\top(t)\boldsymbol{h}(t) + x_{r,3}\right].$$

The last error signal is defined as $e_3(t) = \mu_2(t) - \sigma_1(t)$, where $\sigma_1(t)$ is generated by the system

$$\begin{aligned} \dot{\sigma}_1(t) &= \omega\sigma_2(t) \\ \dot{\sigma}_2(t) &= -2\zeta\omega\sigma_2(t) - \omega[\sigma_1(t) - \alpha_2(t)]\,. \end{aligned} \tag{50}$$

This reduces the error dynamics (49) into

$$\dot{e}_2(t) = -e_1(t) - c_2 e_2(t) + \hat{b}(t)e_3(t) + \hat{b}(t)\left[\sigma_1(t) - \alpha_2(t)\right] + (\lambda + c_1)\tilde{z}_2(t)\,. \tag{51}$$

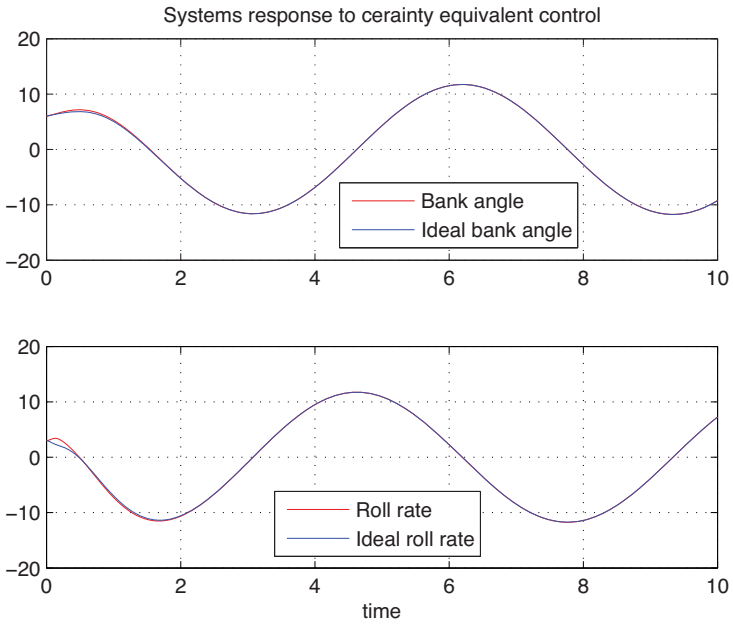

Figure 5. Sinusoidal response to the certainty equivalent control.

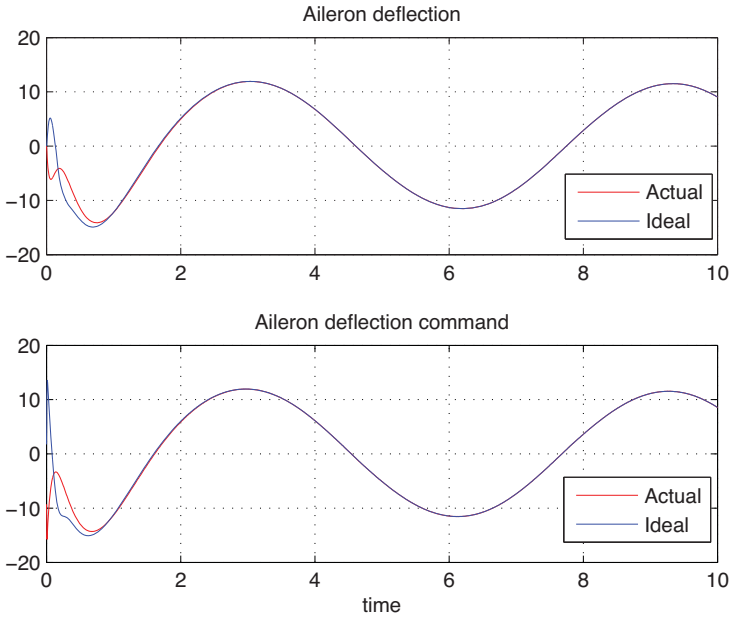

Figure 6. Actual aileron deflection and certainty equivalent adaptive control signal vs ideal ones for the sinusoidal command.

The control signal is defined as

$$u(t) = -\hat{b}(t)e_2(t) - c_3e_3(t) + k_{02}\mu_1(t) - \omega\sigma_2(t),$$

which reduces the dynamics of $e_3(t)$ into

$$\dot{e}_3(t) = -\hat{b}(t)e_2(t) - c_3e_3(t) \tag{52}$$

We test the algorithm in simulations for the wing rock model from Ref.[9] with $\theta_1 = -0.0186$, $\theta_2 = 0.0152$,

$\theta_3 = -0.0625$, $\theta_4 = 0.0095$, $\theta_5 = 0.0215$, $b_a = 1$ and $\tau = 1/15$. We choose $\boldsymbol{k}_0 = [3\ 2]^\top$ for the filtered input and output transformation. For the reference model we set $\boldsymbol{k} = [4.86\ 7.56\ 4.38]^\top$ and $k_r = 4.86$]. The command filtering is implemented with $\omega = 500$ and $\zeta = 0.8$. We run simulations from the initial conditions $\phi(0) = 6deg,\ p(0) = 3deg/sec,\ \delta_a(0) = 0deg$. The adaptation rate is set to $\gamma = 25000$ with $\lambda = 2\sqrt{\gamma}$, and the control gains are set to $c_1 = c_2 = c_3 = 2$. The lower bound for $\hat{b}(t)$ is set to 0.01.

Figure 1 displays the tracking performance of the ideal command filtered output feedback backstepping control for the bank angle step command of magnitude 15 deg, assuming that the parameters are known to the controller. The performance of the certainty equivalence control with respect to the ideal response is presented in Figure 2, and the corresponding aileron deflections and commands to the aileron actuators are presented in Figure 3. It can be seen that the presented output feedback M-MRAC achieves good tracking performance for both output and control signals.

Next set of figures (Figures 4,5 and 6) represent the systems performance for the sinusoidal external command of magnitude 15 deg and frequency of $1rad/sec$. Figure 4 displays the tracking performance of the ideal controller with respect to the reference model, and Figure 5 displays the performance of the certainty equivalent control with respect to ideal one. Again, it can be observed that the M-MRAC exhibits adequate behavior as in output tracking, as well as in the input tracking which is apparent from Figure 6.

B. Control of Short Period Dynamics

As an example we consider the longitudinal control of a damaged transport class model (TCM) as defined in Ref.[3] The short period dynamics of the GTM can be represented as (see for example Ref.[12] for definitions)

$$\begin{aligned} \dot{\alpha}(t) &= \frac{Z_\alpha}{V}\alpha(t) + \left(1 + \frac{Z_q}{V}\right) q(t) \\ \dot{q}(t) &= M_\alpha \alpha(t) + M_q q(t) + M_{\delta_e}\delta_e(t)\,, \end{aligned} \tag{53}$$

where α is the angle of attack, q is the pitch rate and δ_e is the elevator deflection, the simplified dynamics of which are modeled as a first order system

$$\dot{\delta}_e(t) = k_e\left[u(t) - \delta_e(t)\right]\,, \tag{54}$$

where $u(t)$ is the control input to the elevator actuator, k_e is the actuator's gain. We assume that the controlled output is the pitch rate, which is the only measurement available for feedback.

Deriving the transfer function from u to q we obtain

$$G_{uq}(s) = \frac{k_e s - k_e \frac{Z_\alpha}{V}}{s^3 + \left(k_e - M_q - \frac{Z_\alpha}{V}\right)s^2 + \left[M_q\frac{Z_\alpha}{V} - M_\alpha\left(1 + \frac{Z_q}{V}\right) - k_e\left(M_q + \frac{Z_\alpha}{V}\right)\right]s + k_e\left[M_q\frac{Z_\alpha}{V} - M_\alpha\left(1 + \frac{Z_q}{V}\right)\right]}\,,$$

therefore the system can be easily transformed into the observer form

$$\begin{aligned} \dot{x}_1(t) &= x_2(t) + \theta_1 x_1(t) \\ \dot{x}_2(t) &= x_3(t) + \theta_2 x_1(t) + b_1 u(t) \\ \dot{x}_3(t) &= \theta_3 x_1(t) + b_0 u(t) \end{aligned} \tag{55}$$

$$y(t) = x_1(t)\,, \tag{56}$$

where the form of the unknown parameters $\theta_1 = k_e - M_q - \frac{Z_\alpha}{V}$, $\theta_2 = M_q\frac{Z_\alpha}{V} - M_\alpha\left(1 + \frac{Z_q}{V}\right) - k_e\left(M_q + \frac{Z_\alpha}{V}\right)$, $\theta_3 = k_e\left[M_q\frac{Z_\alpha}{V} - M_\alpha\left(1 + \frac{Z_q}{V}\right)\right]$, $b_1 = k_e$ and $b_0 = -k\frac{Z_\alpha}{V}$. Following Ref.[6] (p. 421) we use the input and output filters for the special case of linear systems

$$\dot{\boldsymbol{s}}_u(t) = A_0\boldsymbol{s}_u(t) + \begin{bmatrix} 0 \\ 0 \\ 1 \end{bmatrix} u(t)\,, \quad \dot{\boldsymbol{s}}_y(t) = A_0\boldsymbol{s}_u(t) + \begin{bmatrix} 0 \\ 0 \\ 1 \end{bmatrix} y(t), \quad A_0 = \begin{bmatrix} -k_{0,1} & 1 & 0 \\ -k_{0,2} & 0 & 1 \\ -k_{0,3} & 0 & 0 \end{bmatrix} \tag{57}$$

to generate vectors $\boldsymbol{w}_j(t) = A_0^j\boldsymbol{s}_u(t),\ j = 0, 1,\ \boldsymbol{s}(t) = A_0^n\boldsymbol{s}_y(t)$ and $\boldsymbol{\xi}_j(t) = A_0^j\boldsymbol{s}_y(t),\ j = 0, 1, 2$ and the matrix $\Xi(t) = [\boldsymbol{\xi}_2(t)\ \boldsymbol{\xi}_1(t)\ \boldsymbol{\xi}_0(t)]$. Then the system (55) can be written as

$$\begin{aligned} \dot{y}(t) &= b_1 w_{1,2}(t) + s_2(t) + \boldsymbol{h}^\top(t)\boldsymbol{\vartheta} \\ \dot{w}_{1,2}(t) &= u(t) + w_{1,3}(t) - k_{0,2}w_{1,1}(t)\,, \end{aligned} \tag{58}$$

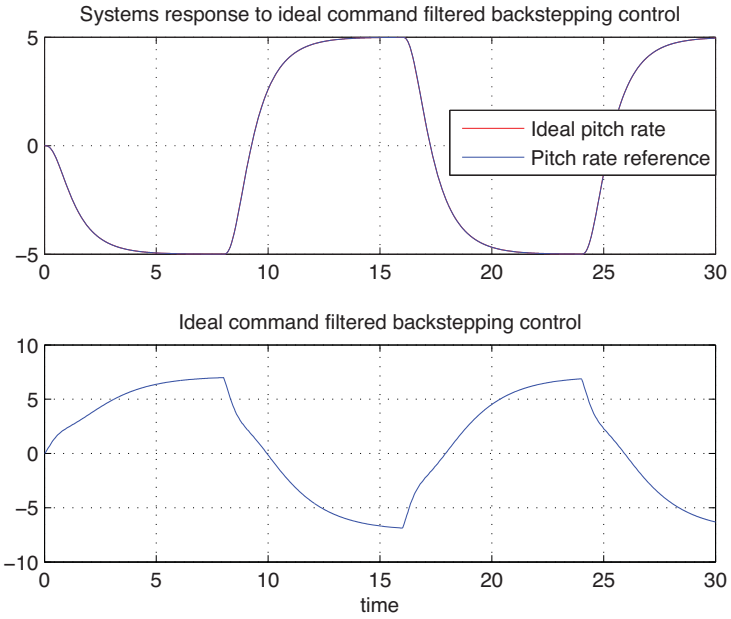

Figure 7. Ideal pitch rate response and ideal command filtered output feedback control.

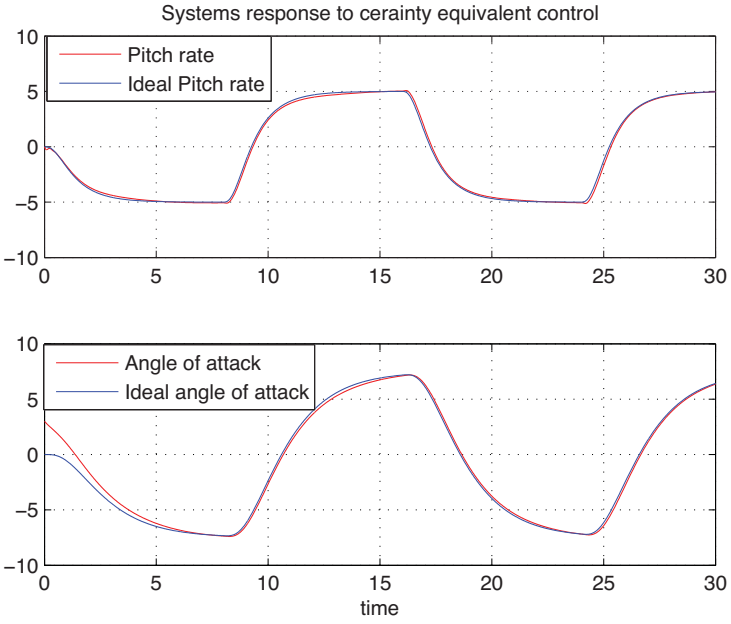

Figure 8. Pitch rate response and the corresponding angle of attack.

where $\boldsymbol{h}^\top(t) = [w_{0,2}(t) \;\; \Xi_{(2)} + y(t)[1\ 0\ 0]]$, and $\boldsymbol{\vartheta} = [b_0\ \theta_1\ \theta_2\ \theta_3]^\top$. The system is now in the from (7), therefore the presented output feedback M-MRAC can be applied.

For the simulation the numeric values of matrices A and B are computed using the vortex-lattice method (see Ref.[7] for details), for the straight level flight condition at an altitude of $30000ft$ and a cruise speed of $0.8M$

The damage scenario corresponds to 60% loss of the left horizontal tail, which roughly corresponds to 59% loss of pitch control effectiveness, 67% loss of pitch damping and 59% loss of pitch stiffness. It is assumed

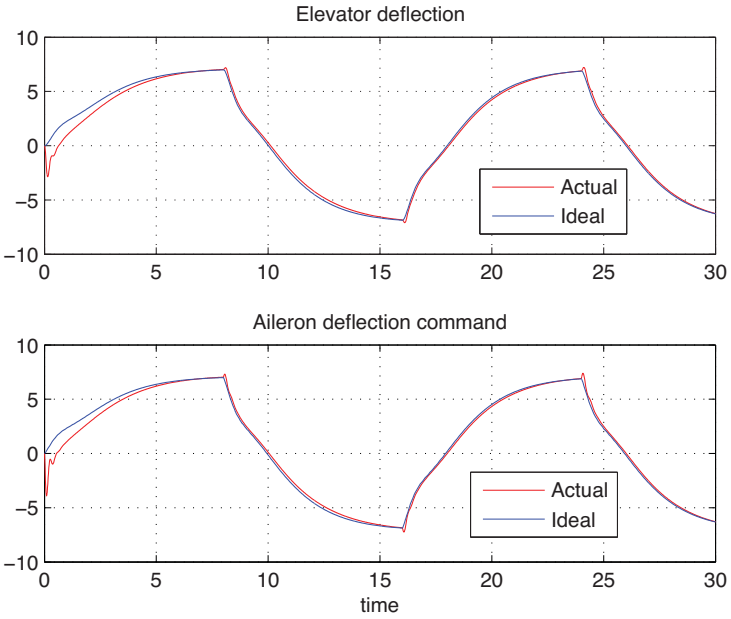

Figure 9. Actual elevator deflection and certainty equivalent adaptive control signal vs ideal ones.

that the aircraft was in steady level flight condition at an altitude of $30000ft$ and a cruise speed of $0.8M$ before the failure.

We choose $\boldsymbol{k}_0 = [6\ 11\ \ 6]^\top$ to generate $A0$, a unity gain second order reference model with frequency of 2.5 and damping ratio of 0.8 and implement the command filtering with a filter, which has $\omega = 300$ and $\zeta = 0.8$. We run simulations from the initial conditions $q(0) = 0deg/sec,\ \alpha(0) = 3deg,\ \delta_e(0) = 0deg$. The adaptation rate is set to $\gamma = 15000$ with $\lambda = 2\sqrt{\gamma}$, and the control gains are set to $c_1 = c_2 = 0.5$. The upper bound for $\hat{b}_1(t)$ is set to -0.01 (b_1 is known to be negative). The external command is a square wave of magnitude 5 deg/sec and of frequency $\pi/8$ rad/sec. In order to make the command differentiable, it is filtered trough a first order filter $\frac{1}{s+1}$.

Figure 7 represents the tracking performance and the ideal command filtered output feedback backstepping control signal. The first plot of Figure 8 displays the output tracking performance of the certainty equivalence M-MRAC with respect to the ideal response. It can be observed that M-MRAC provides a good output tracking. The second plot in the same figure displays the time history of the angle of attack. It can be seen that it closely follows the one generated trough the ideal control. The corresponding elevator deflection and the control input to the actuator are presented in Figure 9. It is seen that the output feedback M-MRAC achieves good tracking for the control signal as well.

VI. Concluding remarks

We have presented an adaptive output feedback backstepping control method for nonlinear systems with unmatched uncertainties that follows the certainty equivalence principle without over-parametrization. The approach uses a fast identification model, which is independent of the control design. This separation of the parameter estimation and control design enables the designer to achieves desired transient and steady state properties. In the control design process we utilize the command filtered backstepping approach. The presented method was applied to two aerospace control problems with good results.

References

[1]J. D. Boskovic and Z. Han. Certainty Equivalence Adaptive Control of Plants With Unmatched Uncertainty Using State Feedback. *IEEE Transactions on Automatic Control*, 54(8):1918 – 1924, 2009.

[2]J. A. Farrell, M. Polycarpou, M. Sharma, and W. Dong. Command Filtered Backstepping. *IEEE Transactions on*

Automatic Control, 54(6):1391–1395, June 2009.

[3]R. M. Hueschen. Development of the Transport Class Model (TCM) Aircraft Simulation From a Sub-Scale Generic Transport Model (GTM) Simulation. *NASA/TM 2011-217169*, August 2011.

[4]H.K. Khalil. *Nonlinear Systems, Third Edition*. Prentice Hall, New Jersey, 2002.

[5]G. Kreisselmeier. An Adaptive Observer with Exponential Rate of Convergence. *IEEE Transactions on Automatic Control*, AC-22:2–8, 1977.

[6]M. Krstic, I. Kanellakopoulos, and P. Kokotovic. *Nonlinear and Adaptive Control Design*. John Wiley & Sons, New York, 1995.

[7]N. Nguyen, K. Krishnakumar, J. Kaneshige, and P. Nespeca. Flight Dynamics and Hybrid Adaptive Control of Damaged Aircraft. *AIAA Journal of Guidance, Control, and Dynamics*, 31(3):751–764, 2008.

[8]J. B. Pomet and L. Praly. Adaptive Nonlinear Regulation: Estimation from the Lyapunov Equation. *IEEE Trans. Autom. Contr.*, 37(6):729–740, 1992.

[9]S. N. Singh, W. Yim, and W. R. Wells. Direct Adaptive and Neural Control of Wing-Rock Motions of Slender Delta Wings. *AIAA Journal of Guidance, Control, and Dynamics*, 18(1):25–30, 1995.

[10]V. Stepanyan and K. Krishnakumar. M-MRAC for Nonlinear Systems with Bounded Disturbances. *In Proc. of the IEEE Conference on Decision and Control, Orlando, FL*, 2011.

[11]V. Stepanyan and K. Krishnakumar. Certainty Equivalence M-MRAC for Systems with Unmatched Uncertainties. *In Proc. of the IEEE Conference on Decision and Control, Maui, HI*, 2012.

[12]B. L. Stevens and F. L. Lewis. *Aircraft Control and Simulaion*. John Wiley & Sons, New York, 1992.